

3D Simulation of Electron Beam Squeezed-State Generation in a Two-Section Drift Tube and Analysis of Its Characteristics

A. G. Petrik^a, S. A. Kurkin^{a,b}, A. A. Koronovskii^{b,a}, and A. E. Hramov^{a,b*}

^a Yuri Gagarin State Technical University of Saratov, Saratov, 410054 Russia

^b Chernyshevsky Saratov State University, Saratov, 410012 Russia

*e-mail: hramovae@gmail.com

Received March 24, 2016

Abstract—A 3D numerical electromagnetic simulation of a vircator in the mode of electron-beam squeezed-state generation is performed. Detailed numerical investigations are carried out, and the dynamics of charged particles in the squeezed state is analyzed. It is shown that the electron beam density (and, as a consequence, effective beam plasma frequency) can be significantly increased in the squeezed state. Hence, the vircator generation frequency and power can also be increased.

DOI: 10.1134/S1063785016080149

Electronic devices with a virtual cathode (VC)—vircators—are of great interest as promising sources of superpower microwave radiation for modern high-power electronics [1–3]. Examples of VC systems that are widely applied in practice are pulsed generators of high-power electromagnetic radiation [2, 4], generators of broadband noise-like oscillations [1, 5], high-power switchers [5], ion accelerators [6], and high-power microwave amplifiers [7]. Therefore, the study of the physical processes occurring in charged-particle beams formed in VC systems is urgent both from the point of view of fundamental problems of plasma physics (concerning various instabilities of charged-particle beams) and that of practical application of the results to optimize the processes in high-power electronic devices.

Note that VC electron beams demonstrate various nonlinear effects, in particular, chaotic dynamics and turbulence [1, 2]. Currently, the possibility of forming the beam squeezed state (BSS) in a VC system is of particular interest. The BSS was observed for the first time in a two-section vircator in [8], where it was shown that some part of electrons are reflected off from the VC formed at the interface between the two sections (the interaction region length undergoes a jump at this interface and, therefore, the critical beam current sharply changes [1]). As a result, a two-beam state is formed in the two-section vircator between the anode and VC. This state is transformed into a squeezed state, considered as a spatially distributed VC. The easiest way to find the BSS is to analyze beam phase portraits at different instants: after a certain instant, the forward and backward beams are closed up along the velocity axis, and one can observe a closely

squeezed electron cloud, resembling a VC distributed over the drift space [8–10]. This state is characterized by high density of electrons with relatively low velocities; in addition, this region contains metastable particles drifting at close-to-zero velocities. In due course, longitudinal space charge oscillations occur between the cathode and VC in the BSS [9]. It should also be noted that complex irregular dynamics of particle motion (up to random) can be observed in the squeezed-state region [8, 10].

In this paper, we report the results of studying the BSS characteristics in a system with a two-section drift space. Specifically, we analyzed and compared the densities and effective plasma frequencies of electron beams in a two-section vircator with a BSS and in a single-section system without a BSS.

The nonlinear time-dependent processes of BSS formation were numerically simulated using the licensed program product CST Particle Studio (CST PS). The CST PS package is widely used for three-dimensional electromagnetic numerical simulation of the processes occurring in electronic devices of different types [11–14]. This package implements a self-consistent model, which simulates the relativistic beam dynamics with the aid of the large-particle method and electromagnetic field dynamics by solving the complete system of Maxwell's equations.

Analysis was performed for a model with a two-section drift space: two butt-jointed tubes of different diameters (Fig. 1). A similar model was used in [8]. Here, the electron source is cylindrical cathode 1, positioned coaxially with the first section of the drift space 3. A voltage applied to anode grid 2 accelerates electrons emitted by the cathode. It was assumed that

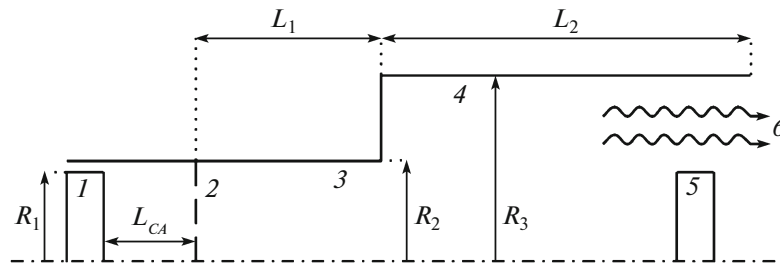


Fig. 1. Schematic diagram of the system under study: (1) cathode, (2) anode grid, (3) anode section, (4) drift section, (5) collector, and (6) microwave power output. The geometric parameters of the system are $L_1 = 70$ mm, $L_2 = 100$ mm, $R_1 = 24$ mm, $R_2 = 27$ mm, and $R_3 = 50$ mm.

the anode grid is completely transparent and that charged particles pass through it without loss. The voltage pulse amplitude and rise time are chosen to be 500 kV and 3 ns, respectively. The beam transmitted through the VC arrives at electron collector 5. Coaxial waveguide 6 is used to extract electromagnetic power; the collector is the central conductor of this waveguide. The entire system is placed in an external longitudinal uniform magnetic field with induction $B = 50$ kG to retain and focus the electron beam. The main control parameter of this system is distance L_{CA} from

the cathode to the anode grid, which can be varied in the range of 10–20 mm by removing the cathode from the anode grid.

The main results of the numerical analysis of the above-described configuration are as follows. After injecting the beam into the two-section vircator, a BSS is formed in the system, which is characterized by a large number of drifting charged particles with close-to-zero velocities (Fig. 2a shows the particle-velocity distribution in the BSS region); specifically these particles facilitate the formation of an ultrahigh-density bunch in the BSS region. In addition, there are metastable particles, which oscillate jointly with the VC during several periods, after which they pass through the VC or return to the squeezed-state region.

After the BSS is settled, the continuous charged-particle beam takes a shape of a hollow cylinder under the action of space charge forces (Fig. 2b shows the averaged radial distribution of space charge density). The appearance and shape of the beam change only slightly in view of its focusing in the strong external longitudinal magnetic field.

The effective plasma beam frequency in the BSS region was calculated according to the formula

$$\langle f_p \rangle_R = \frac{1}{2\pi} \sqrt{\frac{\langle \rho \rangle_R e}{m_r \epsilon_0}},$$

where e is the elementary charge, m_r is the relativistic electron mass, ϵ_0 is the permittivity of free space, and $\langle \rho \rangle_R$ is the radially averaged charge density.

Figure 3 shows the dependences of the effective plasma frequency (determined by the local space charge density in the system) on the longitudinal coordinate for a two-section vircator with a BSS implemented and for a single-section drift space without a BSS, as well as characteristic beam phase portraits for the two-section drift space in the “longitudinal coordinate z –longitudinal beam velocity v_z ” coordinates for different characteristic values of the control parameter: cathode–anode distance L_{CA} . Having compared the two-section system with a system of constant radius (where BSS is not formed), one can conclude that, at the same value of the control param-

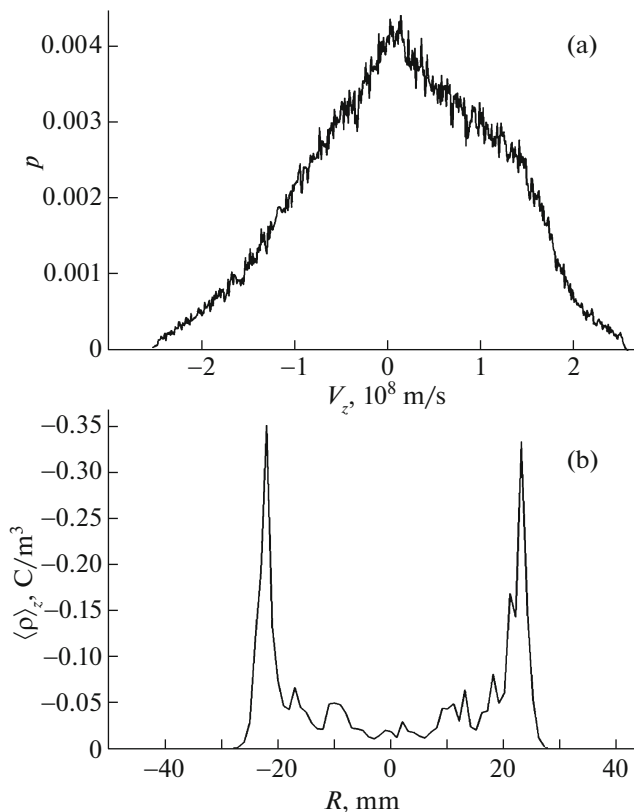


Fig. 2. (a) Particle longitudinal velocity distribution p and (b) the radial dependence of the space charge density averaged over longitudinal coordinate.

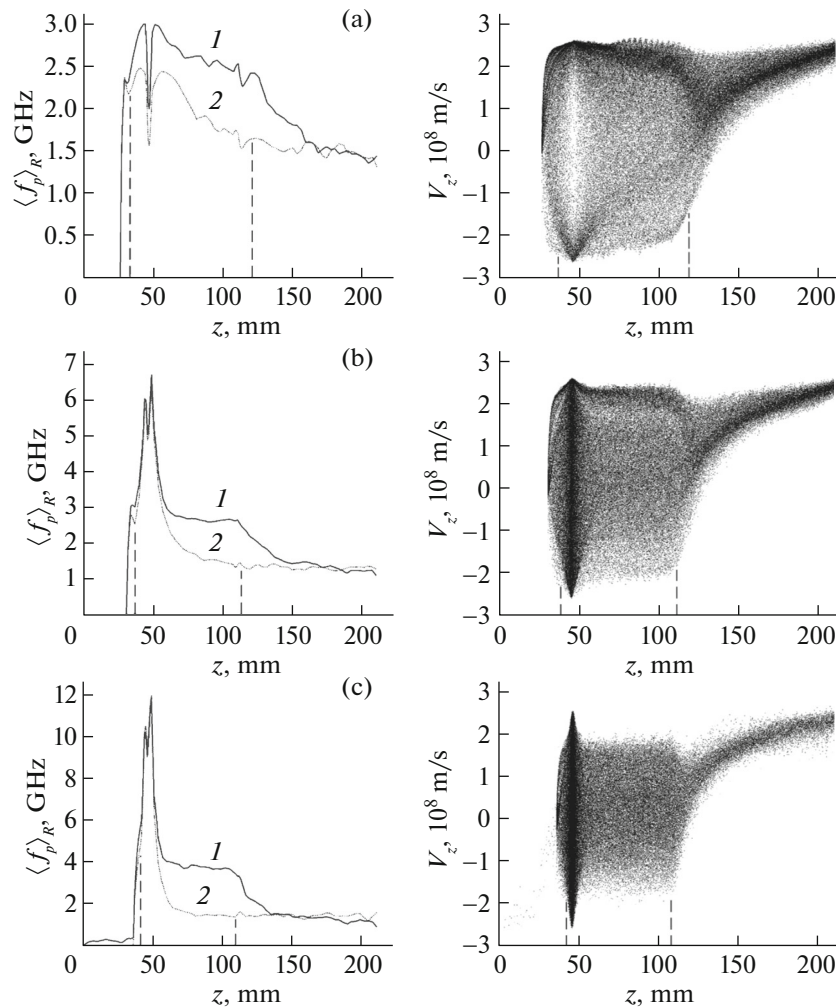


Fig. 3. Ratios of the radially averaged plasma frequencies to the longitudinal coordinate for (1) a two-section system with a BSS and (2) a single-section system without BSS (the tube radius in the BSS-free system is $R = 50$ mm; vertical dotted lines limit the squeezed-state region) and beam phase portraits for the two-section interaction space. Control parameter L_{CA} is (a) 20, (b) 15, and (c) 10 mm.

eter (and, therefore, the same beam current injected into the interaction space), implementation of BSS leads to an approximately twofold increase in the space charge density and plasma frequency in the BSS region (compare curves 1 and 2 in Fig. 3).

At $L_{CA} = 20$ mm (Fig. 3a), the beam phase portrait exhibits a low-density electron cloud, the beam current in the system is still insufficiently close to the critical current for the BSS formation, and the forward and backward beams are not closed up completely. Near the anode grid, one can see a region free of delayed particles; this feature can also be easily found in the dependence of the effective plasma frequency, which exhibits a drop near the anode grid.

A decrease in control parameter L_{CA} to 10 mm (with the corresponding increase in the injected current) leads to a rise in the effective plasma frequency in the region of the first section of smaller radius. Simul-

taneously, the ratio of the plasma frequencies in the systems with and without BSS increases, which is illustrated well by the dependences in Figs. 3b and 3c. Thus, an increase in the beam current causes an increase in the electron cloud density in the BSS region. This rise is due to the observed decrease in the average longitudinal beam velocities in the squeezed-state region (formation of a distributed VC). Simultaneously, the density of accumulated space charge significantly increases near the anode grid, which is evidenced by the peak in the dependence of effective plasma frequency in Figs. 3b and 3c. This effect is not observed in the single-section drift space.

With a further decrease in the cathode–anode distance (and corresponding increase in the beam current), the ratio of the space charge density in the BSS region (which is proportional to the effective plasma frequency) to the charge density in the unperturbed

beam at the input of the first section of the drift space continues to rise.

To analyze the vibrational characteristics in the system, we investigated the time dependences of electric field oscillations in the squeezed-state region for different control parameter values. Based on the temporal realizations of electric field oscillations, we plotted the oscillation power spectra. Note that the typical output spectrum in the BSS mode is noisy and has a weak irregularity; the range of generated frequencies is 0.5–12 GHz. At the same time, there are several pronounced peaks corresponding to the typical values of effective plasma beam frequency. The strongest spectral power peak is observed in the frequency range of 5–6 GHz, which corresponds to approximately doubled effective plasma frequency in the BSS region. The output signal bandwidth tends to rise with an increase in space charge density in the BSS region.

Thus, we analyzed the characteristics of the squeezed state in the two-section drift space of virator. Numerical simulation showed that the system under study contains metastable particles and particles drifting at very low (close-to-zero) velocities. The electric field oscillation spectrum in the squeezed-state region is noisy. Based on the results obtained, one can conclude that a dense hollow electron beam is formed in the system with a two-section drift space in the squeezed-state region; this is a favorable condition for increasing the effective plasma frequency and generation power in this system.

Acknowledgments. The study of the squeezed-state characteristics was supported by the Russian Science Foundation, grant no. 14-12-00222. The development of the model of squeezed-state system was supported by the Ministry of Education and Science of the Russian Federation (projects nos. 3.59.2014/K and 931) and the Russian Foundation for Basic Research (project no. 14-02-31149).

REFERENCES

1. D. I. Trubetskov and A. E. Khramov, *Lectures on Microwave Electronics for Physicists* (Fizmatlit, Moscow, 2003–2004), Vols. 1, 2 [in Russian].
2. A. E. Dubinov and V. D. Selemir, *Radiotekh. Elektron.* **47** (6), 575 (2002).
3. J. Benford, J. A. Swegle, and E. Schamiloglu, *High Power Microwaves*, 3rd ed. (CRC Press, Taylor and Francis, 2015).
4. S. A. Kurkin, A. E. Hramov, and A. A. Koronovskii, *Appl. Phys. Lett.* **103**, 043507 (2013).
5. A. E. Hramov, A. A. Koronovskii, and S. A. Kurkin, *Phys. Lett. A* **374** (30), 3057 (2010).
6. A. E. Dubinov, I. Yu. Kornilova, and V. D. Selemir, *Phys. Usp.* **45** (11), 1109 (2002).
7. S. A. Kurkin, N. S. Frolov, A. O. Rak, A. A. Koronovskii, A. A. Kuraev, and A. E. Hramov, *Appl. Phys. Lett.* **106**, 153503 (2015).
8. A. M. Ignatov and V. P. Tarakanov, *Phys. Plasmas* **1** (3), 741 (1994).
9. E. N. Egorov, A. A. Koronovskii, S. A. Kurkin, and A. E. Hramov, *Plasma Phys. Rep.* **39** (11), 925 (2013).
10. A. E. Dubinov, I. A. Efimova, I. Yu. Kornilova, S. K. Saikov, V. D. Selemir, and V. P. Tarakanov, *Fiz. Elem. Chastits At. Yadra* **35** (2), 462 (2004).
11. M. Einat, M. Pilosof, R. Ben-Moshe, H. Hirshbein, and D. Borodin, *Phys. Rev. Lett.* **109**, 185101 (2012).
12. S. A. Kurkin, A. A. Badarin, A. A. Koronovskii, and A. E. Hramov, *Phys. Plasmas* **22**, 122110 (2015).
13. M. C. Balk, *Proc. IEEE Int. Vacuum Electron. Conf. (IVEC-2008)*, p. 459.
14. A. A. Badarin, S. A. Kurkin, A. A. Koronovskii, and A. E. Hramov, *Tech. Phys. Lett.* **41** (12), 1148 (2015).

Translated by Yu. Sin'kov